Evolution of enzyme catalysts caged in biomimetic gel-shell beads

Fischlechner, Martin ; Schaerli, Yolanda ; Mohamed, Mark F ; Patil, Santosh ; Abell, Chris ; Hollfelder, Florian

Abstract: Natural evolution relies on the improvement of biological entities by rounds of diversification and selection. In the laboratory, directed evolution has emerged as a powerful tool for the development of new and improved biomolecules, but it is limited by the enormous workload and cost of screening sufficiently large combinatorial libraries. Here we describe the production of gel-shell beads (GSBs) with the help of a microfluidic device. These hydrogel beads are surrounded with a polyelectrolyte shell that encloses an enzyme, its encoding DNA and the fluorescent reaction product. Active clones in these man-made compartments can be identified readily by fluorescence-activated sorting at rates >107 GSBs per hour. We use this system to perform the directed evolution of a phosphotriesterase (a bioremediation catalyst) caged in GSBs and isolate a 20-fold faster mutant in less than one hour. We thus establish a practically undemanding method for ultrahigh-throughput screening that results in functional hybrid composites endowed with evolvable protein components.

DOI: https://doi.org/10.1038/nchem.1996

Evolution of Catalysts Caged in Biomimetic Gel-Shell Beads

Martin Fischlechner,[1,2,†] Yolanda Schaerli,[1,2] Mark F. Mohamed,[1] Santosh Patil,[2] Chris Abell,[2] Florian Hollfelder[1*]

[1]Department of Biochemistry, University of Cambridge, Cambridge CB2 1GA, United Kingdom.

[2]Department of Chemistry, University of Cambridge, Lensfield Road, Cambridge CB2 1EW, United Kingdom.

[†]Current address: Institute for Life Sciences, University of Southampton, Southampton, SO17 1BJ, United Kingdom.

*Correspondence to fh111@cam.ac.uk.

Abstract

Natural evolution relies on improvement of biological entities by rounds of diversification and selection. In the laboratory, directed evolution has emerged as a powerful tool for the development of new and improved biomolecules, but is limited by the enormous workload of screening sufficiently large combinatorial libraries and the high costs involved. We present a solution to this problem by creating gel-shell beads (GSBs), biomimetic materials as man-made counterparts to cellular compartments. Generated in microfluidic devices, GSBs consist of a hydrogel bead with a surrounding polyelectrolyte shell that cages an enzyme and its encoding DNA (obtained from *in situ* lysis of a single *E. coli* cell), thus forming a compartment with evolvable parts. The improvement of these hybrid biomaterials by directed evolution is demonstrated for a caged phosphotriesterase (PTE), a bioremediation catalyst, for which a 20-fold faster mutant was isolated from a $5x10^5$-membered library in less than one hour using a standard flow cytometer. We thus establish a practically undemanding method for ultrahigh-throughput screening that results in functional hybrid composites endowed with evolvable protein components.

The prospect of emulating aspects of biological processes in man-made, purpose-built entities has fuelled attempts to design and build functional miniaturized biomimetic assemblies [3,4]. For example, compartments can be built from scratch as mimics that resemble cells in their ability to control access by a semipermeable perimeter compartmentalizing multiple components. Means to construct such functional systems are provided, for example, by polyelectrolyte multilayer technology that is based on the stepwise adsorption of oppositely charged poly-ions on templates [5,6], so that semipermeability and selective retention of cell-like compartments can be rationally engineered [7-13]. Nature relies on Darwinian evolution to create or improve functional molecules. In the laboratory, the equivalent of this process is the combinatorial method of directed evolution that has successfully complemented approaches relying primarily on design [1,2]. In the present work, we demonstrate directed enzyme evolution in polyelectrolyte multilayer compartments (gel-shell beads, GSBs) that can be endowed with genetic information. In order to perform iterative rounds of selection, it is essential to maintain a linkage between the catalyst-encoding DNA (genotype) and the reaction product (phenotype), so that the sequence of the catalyst variants with faster product formation can be retrieved. Establishing a genotype-phenotype linkage turns GSBs into evolutionary units that can be subjected to cycles of randomization, selection and recovery of the code that describes their content. Directed evolution is crucially dependent on screening large numbers of library members in high-quality quantitative enzyme assays as a basis for selecting clones that satisfy a desired criterion: this technical challenge has led to a number of solutions [14-16], but none of them are inexpensive and straightforward. Although design of focused libraries, analysis of mechanism, sequence and structure or adaptation of evolutionary strategies can increase the chances of success of a directed evolution campaign[17-19], the combinatorial diversity of proteins leads to a vast sequence space. Screening a larger number of library members invariably increases the probability of identifying hits. Therefore large screening facilities are often necessary to find catalysts in large libraries. To establish a more convenient format for this perennial problem we have developed an approach that generates ~10^7 identical, monodisperse GSBs per hour, each containing a

protein mutant and its coding DNA. The GSBs can be screened and selected using a widely available benchtop fluorescence-activated cell sorter (FACS).

Results

The target of our directed evolution is the phosphotriesterase (PTE) from *Pseudomonas Diminuta,* an enzyme that detoxifies hazardous pesticides and nerve gas agents by hydrolysis [20,21]. By successful application of GSBs as vehicles for directed enzyme evolution of PTE, we establish the principles behind this approach and demonstrate its utility. Figure 1a summarizes how GSBs are templated in water-in-oil emulsion droplets [22,23] that were made monodispersely with a microfluidic droplet generator (Fig. S1, SI) from an aqueous stream containing agarose and the alginate polyanion. Temperature reduction (from 30 °C to 4 °C) solidifies the agarose and yields a gel core within the droplet, which serves as template for shell assembly. Breaking this emulsion in the presence of the polycation poly(allylamine-hydrochloride) (PAH) surrounds the gel particle with a polyelectrolyte shell; alginate and PAH diffuse and form a polyelectrolyte complex surrounding the agarose core (Fig. S2, SI). This shell serves as template for one or more additional polyelectrolyte multilayer coatings (Fig. S3a, SI). The delivery of alginate from the inside of the particle allows for a coating process fast enough to quantitatively retain enclosed compounds (Fig. S3b-d, SI).

To equip GSBs with a gene and its encoded protein for directed evolution (Fig. 1b), one of the aqueous streams of the microfluidic device contains *E. coli* cells harboring the expressed PTE and its encoding plasmid. A second inlet contains a phosphotriester substrate (that reacts to give a fluorescent product) together with a lysis agent. Single occupancy of cells in droplets can be controlled by the cell concentration and follows a Poisson distribution [24]. In the droplet, the two aqueous phases from the separate inlets are mixed, the cells are lysed [25] and the enzyme catalyst is liberated and thus able to react with substrate. The reaction is conducted in emulsion droplets at 30 °C with agarose in its liquid (sol) form (Fig. S4, SI). The reaction time is precisely controlled by heat-inactivation of the enzyme in the emulsion sample at 90 °C

(for 5 minutes). After de-emulsification and shell formation, the polyelectrolyte shell now retains the gel bead content with a molecular weight cut-off ≤2 kD [10] (Fig. S3, SI) compared to ~250 kD for a gel bead without shell [26]. Consequently the enzyme and the plasmid (the latter also retained by the agarose) remain co-encapsulated (Fig. 3b). The same applies to the reaction product, when a substrate linked to an oligonucleotide tag (20 bp) was employed to ensure its retention. Being far from the site of chemical cleavage the tag's effect on enzymatic rate is small (2-fold; the non-enzymatic rate is identical), while it remains part of the product that is captured by the polyelectrolyte shell. Thus genotype and phenotype are maintained together in the GSB. The product retention ensures that variants can be readily selected based on their activity with respect to a chosen threshold by FACS (Figs. S5 and S6, SI). The recovery of the genotype (in the form of high-copy number plasmids) is achieved by disassembly of the polyelectrolyte shell upon short treatment with a solution of pH 12. This pH is higher than the pK_a of the polycation, which is thus partly deprotonated, so that the polyelectrolyte complex disintegrates [27] and the plasmid DNA can be recovered from beads by standard gel-extraction (Fig. S7, SI). After amplification and cloning, the selected variants are ready for another round of screening and/or mutation, or for sequencing.

To demonstrate the utility of GSBs as biomimetic compartments, directed evolution of the pesticide-degrading enzyme phosphotriesterase (PTE) was performed using the tagged substrate triester **1c** that is turned over to the fluorescent product **2c** (Fig. 2a). To quantify the stringency of this new method, the enrichment of active mutants was first characterized in an experiment separating active PTE from an enzyme lacking the desired activity (acylphosphatase, ACP). PTE-encoding *E. coli* cells were diluted 1:10,000 in cells expressing ACP (Fig. S6, SI). This mixture was then carried through two rounds of screening and selection in GSBs. Fig. 2b shows the reversal of a 1:10,000 dilution of PTE to exclusive selection of PTE, giving an enrichment of >100,000-fold in only two rounds. The stringency of such selections can be governed by variation of the time allowed for product formation. Figure 2c displays selection outcomes for a library in which individual mutants were

allowed to react for decreasing times, so that the resulting library displayed a gradually increasing level of activity in response to the raised threshold. Maintaining identical sorting gates, sample aliquots incubated at 30 °C for 9 h and 3 h before heat inactivation were sorted, recloned and the activity of cell lysates was compared using the substrate paraoxon **1a**. The enriched libraries were 40-fold and 110-fold improved with regard to the initial library (for incubation periods of 9 and 3 h, respectively).

Next, actual selections for more active PTE variants were carried out starting from PTE^{R8} (k_{cat}/K_m of 1.1 x 10^5 $M^{-1}s^{-1}$ for paraoxon **1a** [28]). The library contained 5 x 10^5 clones with ~1.5 random mutations/gene (introduced by error-prone PCR). Fig. 2d shows activity distributions (measured by flow cytometry of GSBs) of three sample aliquots of the library stopped (by heat inactivation) after varying incubation periods, demonstrating that the enzyme's fitness landscape (i.e. a distribution function describing the activity of each library member) can be monitored. At this point selection pressure was directly applied by choosing a threshold for a minimal amount of product formed, measured by the fluorescence of GSBs. For example, sorting the library after 1.5 h of incubation time gave 1000 selected clones (0.2% of a library of initially 5 x 10^5 members). The selected library members were recovered, recloned, and 10% of the enriched population assayed with paraoxon **1a** in one 96-well plate. The majority of clones showed improved activity (>2-fold) and one drastically improved variant, PTE^{F9} (containing two mutations, Leu106Ile and a silent mutation in position 238) was identified. Figure 3a shows the kinetic data for the purified PTE^{F9} that is 8-fold improved in k_{cat}/K_m for its native substrate, the pesticide paraoxon **1a** (k_{cat}/K_m ~8.8 x 10^5 M^{-1} s^{-1}) and 19-fold for the substrate tetraethyl-O-fluorescein-diphosphate **1b** (matching the substrate **1c** employed during screening, except for the absence of the oligonucleotide tag) when compared to its parent PTE^{R8}. The improvement is similar, when instead of free enzyme in solution, molecules of PTE are encapsulated in GSBs and used as caged catalysts (Fig. 3b), with PTE^{F9} showing an enhancement of an order of magnitude over its parent. GSBs containing the caged catalysts can be recovered after use, offering the advantages of immobilized enzymes, but without the need for separate expression, purification and surface conjugation [29].

Discussion

Our work establishes GSBs as biomimetic compartments whose content can be modified by directed evolution. Evolution in GSBs shares many of the attractive features of on-chip evolution in microfluidic droplet devices [14,30] - minimal sample consumption per library member in pico- to nanolitre volumes and precision control of droplet size for sensitive quantitative readouts and selection under non-physiological conditions. However, in contrast to transient, fluid droplets in microfluidic devices, the compartmentalization is robustly 'immortalized' in GSBs. The stability of GSBs allows them to be handled and analyzed in aqueous solution by standard FACS equipment (rather than custom-made microfluidic on-chip emulsion sorters [25,31-34]). FACS can also be employed for cell-based selections, but they either rely on *in vivo* live/dead assays [35] or require that the reaction product must be captured in or on cells [36,37].

The artificial compartment – be it droplet or GSB – serves to capture the reaction product, so that reaction progress can be determined. While display systems (such as phage or yeast display) provide ready access to large libraries (and are frequently used for evolution of *binders*), capture mechanisms for reaction product must be introduced to enable selections for multiple turnover *catalysts* [15]. The genotype-phenotype linkage by compartmentalization in GSBs makes product capture more general, based on the adjustable size-selectivity of the shell. This product capture mechanism can be actively controlled by molecule tagging and shell design to set-up selective permeability. While mirroring the role of a natural cell membrane, a man-made product capture system makes selections under *in vitro* conditions possible and the degrees of freedom in the design of selection schemes are increased. Multilayer technology provides versatile means of designing functional enclosures with variations in the building block polyelectrolytes [38], so that GSBs can be used under non-physiological or even extreme conditions: for example, the PAH/PSS (poly(allylamine-hydrochloride)/poly(styrene-sulfonate)) system withstands temperatures up to 95 °C [10], is stable between 2 and pH 11 [27], and capsules can even be filled with organic solvents without losing their integrity [39]. The 'immortalization' of droplets makes GSB compartments also suitable for multi-step processes, in

which small molecules can be exchanged, while the bead shell cages proteins and DNA. While buffer components, reactants, substrates and other small molecules can enter and leave, the evolutionary unit remains intact.

The successful embedding of an enzyme into a composite material endowed with the ability to break down the pesticide paraoxon **1b** (Fig. 3b) provides an example for biodegradation of this compound or related chemical warfare agents using *in vitro* decontamination. GSBs can be seen as materials with caged catalysts for cost effective and sustainable applications that require easy recovery and repeated use of enzymes [29]. The stable catalyst cage of a GSB can contain single proteins, but may also encapsulate multiple components, e.g. sequential enzyme cascades or tandem reactions [40-44], enzymatic pathways [45-47], or synthetic gene circuits [48] that can be evolved directly in this format. The synthesis of biomimetic compartments using materials science technology provides a practically straightforward approach for directed evolution by harnessing the power of ultrahigh-throughput screening in GSBs.

Methods

Production of gel-shell beads in microfluidic devices: Microdroplets were generated in devices fabricated (see SI, Fig. S1) from poly(dimethyl)siloxane (PDMS) using standard soft lithography [49]. Fluorinated oil (3M Novec HFE-7500) with 0.5% (w/w) surfactant (EA-surfactant from Raindance Technologies or a krytox-jeffamine triblock copolymer, see SI) was used as carrier phase. Typically droplets were produced at rate of 2.7 kHz (flow rates of 2 x 15 µL/h for the aqueous phases, 500 µL/h for the oil phase) with a diameter of 18 µm. Solutions of agarose in sol (1.5%, w/v), in 50 mM Tris-HCl pH 7.5, 100 mM NaCl) and sodium-alginate (1.5%, w/v), in Tris-HCl (50 mM, pH 7.5, 100 mM NaCl) were filled into two separate syringes. The remaining aqueous-phase components of the assays were divided into the two syringes depending on their temperature requirement and assay compatibility, e.g.

lysate buffer and substrate in the first syringe and cells in the second. After droplet formation, the resulting droplets contained alginate and agarose (0.75%, w/v). Emulsions were harvested off-chip in Eppendorf tubes with an overlay of mineral oil and cooled on ice for at least 15 min before the conversion to gel-shell beads. A polydisperse emulsion containing the polycation PAH (10 mg/mL in 0.5 M NaCl) in HFE 7500 (0.05% surfactant, w/w) was prepared by vigorous vortexing. 1 mL of this polydisperse emulsion was mixed with 10 µL agarose/alginate-containing monodisperse emulsion and vortexed thoroughly. Then, 500 µL 1H,1H,2H,2H-perfluorooctanol (PFO, 97%, Alfa Aesar) were added and vortexed. After centrifuging the sample for 10 s, the aqueous supernatant containing the GSBs was harvested and washed by centrifugation (2500 g, 5 min) in 100 mM NaCl.

Libraries: Phosphotriesterase (PTE R8) [28] with an N-terminal strep-tag and ACP were inserted into a pRSFDuet vector (Novagen). Libraries were created by error-prone PCR (Mutazyme II, Stratagene) following the manufacturer's instructions. Plasmid preparations of the libraries were transformed into electrocompetent *E. coli* BL21 (DE3). The transformed cells were grown overnight in 10 mL LB containing kanamycin (30 µg/mL), diluted into fresh medium, induced with IPTG (1 mM) after reaching an OD of 0.6 and incubated for another 3 h at 37 ºC. After addition of glycerol (25% v/v) samples were frozen in liquid nitrogen for storage.

Selections: Frozen aliquots of induced *E. coli* BL21 (DE3) cultures harboring ACP, PTE or libraries were thawed on ice and washed 5 times by centrifugation (2 min, 2000 g) with Tris-HCl buffer (pH 7.5, 50 mM supplemented with 100 mM NaCl). Two solutions were prepared: the first containing alginate (1.5%, w/v) and the cells, the second agarose (1.5%, w/v) CellyticB Cell Lysis Reagent (0.1x; Sigma) rLysozyme solution (0.6 ku/µL, Novagen) and the substrate **1c** (30 µM). Droplets were produced as described above and incubated at 30 °C. The enzymatic reaction was stopped by heat inactivation at 95 °C for 5 min. GSBs were produced as described above and coated with a second layer consisting of bovine serum albumin (BSA). A MoFlo cell sorter (Beckman Coulter) equipped with a 70 µm

nozzle was used for sorting. The selected beads were harvested in 50 µL NaCl (100 mM). 50 µL 0.2 M NaOH were added to the sorted sample, vortexed and incubated on a shaker for 5 min at RT. Then, BSA (10 µL; 20 mg/mL in H_2O) and linearized dephosphorylated pUC19 plasmid (100 ng) were added and vortexed, followed by adding acetic acid (5 µL; 2 M). The plasmids were then recovered from the agarose using a plasmid gel extraction kit (Gel Recovery Kit, Zymoclean) and amplified with an isothermal DNA amplification kit (illustra TempliPhi, GE-Healthcare). Finally, the genes were PCR amplified and recloned into the vector backbone.

The experimental methods (including substrate synthesis) are described in extensive detail in the Supplementary Information.

References

1. Turner, N.J. Directed evolution drives the next generation of biocatalysts. *Nat Chem Biol* **5**, 567-73 (2009).
2. Bornscheuer, U.T. et al. Engineering the third wave of biocatalysis. *Nature* **485**, 185-94 (2012).
3. Retterer, S.T. & Simpson, M.L. Microscale and nanoscale compartments for biotechnology. *Curr Opin Biotechnol* **23**, 522-8 (2012).
4. Walde, P. Building artificial cells and protocell models: Experimental approaches with lipid vesicles. *Bioessays* **32**, 296-303 (2010).
5. Decher, G. Fuzzy nanoassemblies: Toward layered polymeric multicomposites. *Science* **277**, 1232-1237 (1997).
6. Donath, E., Sukhorukov, G.B., Caruso, F., Davis, S.A. & Mohwald, H. Novel hollow polymer shells by colloid-templated assembly of polyelectrolytes. *Angewandte Chemie-International Edition* **37**, 2202-2205 (1998).
7. Stadler, B. et al. Polymer hydrogel capsules: en route toward synthetic cellular systems. *Nanoscale* **1**, 68-73 (2009).
8. Tong, W.J., Song, X.X. & Gao, C.Y. Layer-by-layer assembly of microcapsules and their biomedical applications. *Chemical Society Reviews* **41**, 6103-6124 (2012).
9. Peyratout, C.S. & Dahne, L. Tailor-made polyelectrolyte microcapsules: From multilayers to smart containers. *Angewandte Chemie-International Edition* **43**, 3762-3783 (2004).
10. Mak, W.C., Cheung, K.Y. & Trau, D. Diffusion Controlled and Temperature Stable Microcapsule Reaction Compartments for High-Throughput Microcapsule-PCR. *Advanced Functional Materials* **18**, 2930-2937 (2008).
11. Price, A.D., Zelikin, A.N., Wark, K.L. & Caruso, F. A Biomolecular "Ship-in-a-Bottle": Continuous RNA Synthesis Within Hollow Polymer Hydrogel Assemblies. *Advanced Materials* **22**, 720-+ (2010).
12. Baumler, H. & Georgieva, R. Coupled Enzyme Reactions in Multicompartment Microparticles. *Biomacromolecules* **11**, 1480-1487 (2010).

13. Pescador, P., Toca-Herrera, J.L., Donath, E. & Katakis, I. Efficiency of a Bienzyme Sequential Reaction System Immobilized on Polyelectrolyte Multilayer-Coated Colloids. *Langmuir* **24**, 14108-14114 (2008).
14. Schaerli, Y. & Hollfelder, F. The potential of microfluidic water-in-oil droplets in experimental biology. *Mol Biosyst* **5**, 1392-404 (2009).
15. Leemhuis, H., Stein, V., Griffiths, A.D. & Hollfelder, F. New genotype-phenotype linkages for directed evolution of functional proteins. *Curr Opin Struct Biol* **15**, 472-8 (2005).
16. Lin, H. & Cornish, V.W. Screening and selection methods for large-scale analysis of protein function. *Angew Chem Int Ed Engl* **41**, 4402-25 (2002).
17. Jäckel, C. & Hilvert, D. Biocatalysts by evolution. *Curr Opin Biotechnol* **21**, 753-9 (2010).
18. Tracewell, C.A. & Arnold, F.H. Directed enzyme evolution: climbing fitness peaks one amino acid at a time. *Current Opinion in Chemical Biology* **13**, 3-9 (2009).
19. Romero, P.A. & Arnold, F.H. Exploring protein fitness landscapes by directed evolution. *Nat Rev Mol Cell Biol* **10**, 866-76 (2009).
20. Yang, Y., Baker, J.A. & Ward, J.R. Decontamination of Chemical Warfare Agents. *Chem. Rev.* **92**, 1729-1743 (1992).
21. Morales-Rojas, H. & Moss, R.A. Phosphorolytic reactivity of o-iodosylcarboxylates and related nucleophiles. *Chem Rev* **102**, 2497-521 (2002).
22. Tawfik, D.S. & Griffiths, A.D. Man-made cell-like compartments for molecular evolution. *Nat Biotechnol* **16**, 652-6 (1998).
23. Miller, O.J. et al. Directed evolution by in vitro compartmentalization. *Nat Methods* **3**, 561-70 (2006).
24. Huebner, A. et al. Quantitative detection of protein expression in single cells using droplet microfluidics. *Chem Commun (Camb)*, 1218-20 (2007).
25. Kintses, B. et al. Picoliter cell lysate assays in microfluidic droplet compartments for directed enzyme evolution. *Chem Biol* **19**, 1001-9 (2012).
26. Weaver, J.C., Bliss, J.G., Powell, K.T., Harrison, G.I. & Williams, G.B. Rapid clonal growth measurements at the single-cell level - gel microdroplets and flow-Cytometry. *Bio-Technology* **9**, 873-877 (1991).
27. Dejugnat, C. & Sukhorukov, G.B. PH-responsive properties of hollow polyelectrolyte microcapsules templated on various cores. *Langmuir* **20**, 7265-7269 (2004).
28. Tokuriki, N. et al. Diminishing returns and tradeoffs constrain the laboratory optimization of an enzyme. *Nat Commun* **3**, 1257 (2012).
29. Dicosimo, R., McAuliffe, J., Poulose, A.J. & Bohlmann, G. Industrial use of immobilized enzymes. *Chem Soc Rev* **42**, 6437-74 (2013).
30. Theberge, A.B. et al. Microdroplets in microfluidics: an evolving platform for discoveries in chemistry and biology. *Angew Chem Int Ed Engl* **49**, 5846-68 (2010).
31. Ahn, K. et al. Dielectrophoretic manipulation of drops for high-speed microfluidic sorting devices. *Applied Physics Letters* **88**(2006).
32. Baret, J.C. et al. Fluorescence-activated droplet sorting (FADS): efficient microfluidic cell sorting based on enzymatic activity. *Lab on a Chip* **9**, 1850-1858 (2009).
33. Agresti, J.J. et al. Ultrahigh-throughput screening in drop-based microfluidics for directed evolution. *Proc Natl Acad Sci U S A* **107**, 4004-9 (2010).
34. Hawley, T.S. & Hawley, R.G. *Flow Cytometry Protocols*, (Humana Press, 2004).
35. Fernandez-Alvaro, E. et al. A combination of in vivo selection and cell sorting for the identification of enantioselective biocatalysts. *Angew Chem Int Ed Engl* **50**, 8584-7 (2011).
36. Yang, G. & Withers, S.G. Ultrahigh-throughput FACS-based screening for directed enzyme evolution. *Chembiochem* **10**, 2704-15 (2009).

37. Becker, S. et al. Single-cell high-throughput screening to identify enantioselective hydrolytic enzymes. *Angew Chem Int Ed Engl* **47**, 5085-8 (2008).
38. Skirtach, A.G., Yashchenok, A.M. & Mohwald, H. Encapsulation, release and applications of LbL polyelectrolyte multilayer capsules. *Chem Commun (Camb)* **47**, 12736-46 (2011).
39. Moya, S., Sukhorukov, G.B., Auch, M., Donath, E. & Mohwald, H. Microencapsulation of Organic Solvents in Polyelectrolyte Multilayer Micrometer-Sized Shells. *J Colloid Interface Sci* **216**, 297-302 (1999).
40. Schoffelen, S. & van Hest, J.C. Chemical approaches for the construction of multi-enzyme reaction systems. *Curr Opin Struct Biol* **23**, 613-21 (2013).
41. Liu, Y. et al. Biomimetic enzyme nanocomplexes and their use as antidotes and preventive measures for alcohol intoxication. *Nat Nanotechnol* **8**, 187-92 (2013).
42. Oroz-Guinea, I. & Garcia-Junceda, E. Enzyme catalysed tandem reactions. *Curr Opin Chem Biol* **17**, 236-49 (2013).
43. Garcia-Junceda, E. *Multi-Step Enzyme Catalysis: Biotransformations and Chemoenzymatic Synthesis* 256 (VCH, Weinheim, 2008).
44. Ricca, E., Brucher, B. & Schrittwieser, J.H. Multi-Enzymatic Cascade Reactions: Overview and Perspectives. *Advanced Synthesis & Catalysis* **353**, 2239-2262 (2011).
45. Zhang, Y.-H.P. Simpler is better: high-yield and potential low-cost biofuels production through cell-free synthetic pathway biotransformation (SyPaB). *ACS Catal* **1**, 998–1009 (2011).
46. Ro, D.K. et al. Production of the antimalarial drug precursor artemisinic acid in engineered yeast. *Nature* **440**, 940-3 (2006).
47. Pirie, C.M., De Mey, M., Jones Prather, K.L. & Ajikumar, P.K. Integrating the protein and metabolic engineering toolkits for next-generation chemical biosynthesis. *ACS Chem Biol* **8**, 662-72 (2013).
48. Zhao, H. *Synthetic Biology*, (Academic Press, New York City, 2013).
49. Devenish, S.R., Kaltenbach, M., Fischlechner, M. & Hollfelder, F. Droplets as reaction compartments for protein nanotechnology. in *Protein Nanotechnology: Protocols, Instrumentation and Applications*, Vol. 996 (ed. Gerrard, J.) 269-86 (2013).

Acknowledgments

This research was funded by the EPSRC, by EU Marie-Curie fellowships (to MF, MM) and by fellowships from the Schering foundation, the Cambridge Overseas Trust and Trinity Hall (to YS). FH is an ERC Starting Investigator. We thank Nigel Miller for help with FACS and several colleagues or helpful discussions and comments on the manuscript. We thank RainDance Technologies (Lexington, US) for a sample of EA-surfactant.

Author contributions

MF developed the concept, designed, conducted and analyzed the experiments. YS developed the concept, designed, conducted and analyzed preliminary experiments. MF, YS, MM and FH wrote the manuscript. MM and SP synthesized enzyme substrates. FH and CA directed the research.

Additional information

Supplementary information is available in the online version of the paper. Reprints and permissions information is available online at www.nature.com/reprints. Correspondence and requests for materials should be addressed to F.H.

Figures

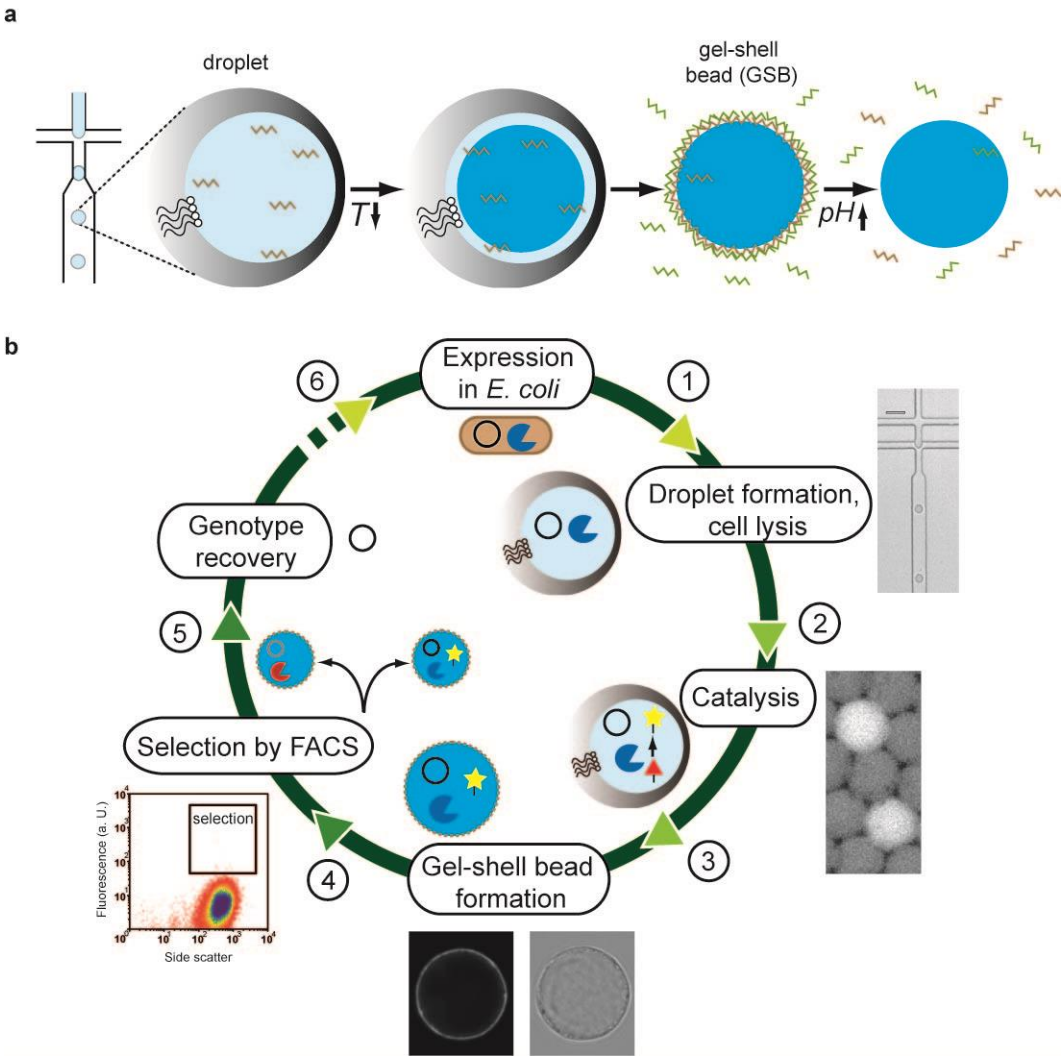

Figure 1: ***Directed evolution in biomimetic gel-shell beads (GSBs).*** **(a)** ***Assembly and structure.*** Monodisperse water-in-oil emulsion droplets are produced with a microfluidic emulsion generator (see SI, Figs. S1 and S2 for details). The aqueous solution from which droplets are derived contains agarose and the polyanion alginate (brown zig-zag line, see also Fig. 3b) that gelate upon cooling (from 30 °C to 4 °C), so that a solid bead is formed within the droplet template. The droplet boundary is removed by breaking the emulsion in the presence of the polycation poly(allylamine hydrochloride (PAH ; green zig-zag line, see also Fig. 3b). Upon spontaneous encounter of the anionic alginate and the cationic PAH at the surface of the agarose template, a polyelectrolyte complex forms that maintains compartmentalization and substitutes the oil/water interface of the former emulsion droplet with a semipermeable surface layer (SI, Fig. S3), functionally resembling a

semipermeable cell membrane. The shell formation is reversible: disassembly readily occurs under basic conditions (SI, Fig. S7).

(b) *Evolution in GSBs*. (1) GSBs are endowed with genetic information by compartmentalizing single *E. coli* cells that are delivered *via* the aqueous phase into the droplet (with Poisson distribution governing the occupancy). Prior to droplet formation, *E. coli* have been induced to express the enzyme. When the cells are lysed upon droplet formation, the enzyme (◔) and its coding plasmid (black circle) are liberated. **(2)** The encounter of enzyme and substrate (**1c**, ▲) leads to formation of a fluorescent product (**2c**,★) and the image shows bright droplets containing active enzyme in contrast to non-fluorescent droplets without it. The time allowed for product formation can be gradually decreased to increase the selection pressure (Fig. 2b). **(3)** When the GSB is formed, the plasmids of a single type remain co-compartmentalized with the protein they encode. The shell further serves to retain the reaction product. As a consequence, GSBs harboring active enzyme are distinguished from those with inactive enzyme variants by their fluorescence. (Images: brightfield and a fluorescence microscopy pictures of a GSB; highlighting the polyelectrolyte shell using a fluorescein-labelled polycation; see SI) **(4)** The identification and isolation of catalytically active hits is performed by FACS (>10^7 in ~10 min). **(5)** In very basic conditions (pH 12) the shell is removed, the coding plasmid is recovered and the selected variants are sequenced or further characterized. **(6)** Alternatively further randomization is performed to generate a new library that is entered into a further round of evolution.

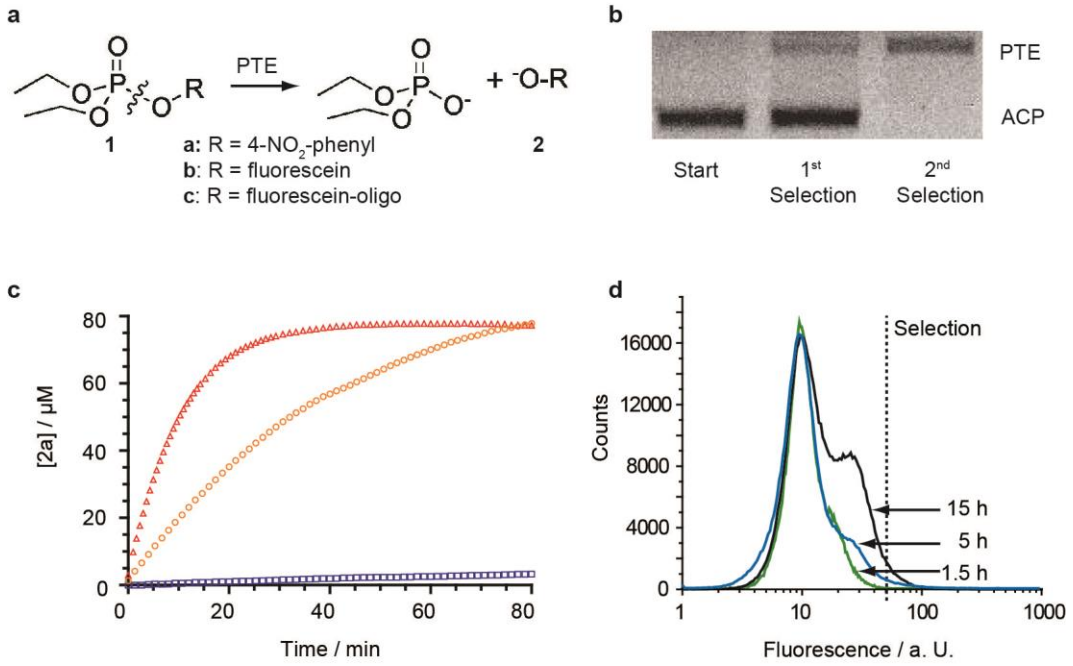

Figure 2. ***Model selections and directed evolution of active PTE in gel-shell beads.*** **(a)** ***Reaction scheme.*** **1a**: paraoxon (native substrate; R=4-nitrophenol) **1b**/**c**: triesters with fluorescent leaving groups, i.e. tetraethyl-O-fluorescein-diphosphate (**1b**) and tetraethyl-O-fluorescein-diphosphate coupled to an oligonucleotide tag (**1c**) that keeps the product **2c** in GSBs (**1c**; used for selections; see SI for detailed structures. The tag has no effect on non-enzymatic hydrolysis and only reduces the enzymatic rate by ~2-fold.) **(b)** **Q*uantification of enrichment*.** A 1:10,000 mixture of the genes coding for active wild-type PTE and an enzyme without activity towards phosphate triesters (ACP, acylphosphatase from *E. coli,* accession number EDX37041) served as the starting point for selections. Prior to selection only the ACP gene (285 bp), but not the PTE gene (1007 bp) is visible on an agarose gel after PCR amplification. Two rounds of selection (as in Figure 1b) reverse this observation dramatically: now the PTE gene dominates and ACP is invisible. **(c)** ***The influence of selection pressure on selection outcome*.** A PTE library (blue squares) was generated by error-prone PCR (7.75 errors/gene, library size: 380,000 members) and incubated for 9 (orange circles) or 3 (red triangles) hours before sorting and selection. The cell lysates of the resulting populations were assayed with paraoxon **1a** in a plate reader. Compared to the initial library, the lysates from libraries sorted after 9 and 3 hours of incubation were 40- and 110-fold, respectively, more active (best 2% and

1.2% of library members were selected, respectively). **(d)** ***Actual selections of improved PTE variants.*** Overlay of the fluorescence distribution with varying incubation times of gated single GSBs harboring a library of ~5 x 10^5 members (derived by error-prone PCR with a mutation frequency of 1.5 mutations/gene from PTE^{R8}). The emerging peak on the right corresponds to an increasing fraction of GSBs with more product as a function of time (15 h black; 5 h blue; 1.5 h green). Thus, the shorter reaction time (1.5 h, green) was used for stringent sample sorting (in which GSBs with fluorescence above the dotted line were selected). 10% of the resulting clones were picked randomly and analyzed in lysate assays in one 96-well plate for turnover of paraoxon **1a** and the best mutant, PTE^{F9} was further characterized (Fig. 3).

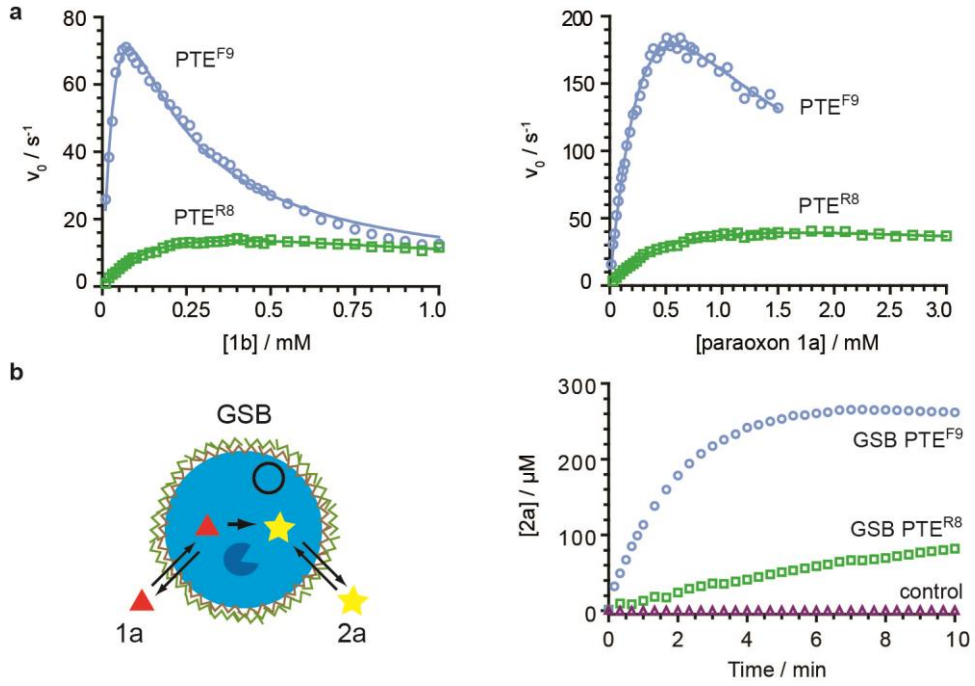

Figure 3. ***Triester hydrolysis by PTE and its evolved variants***. **(a)** ***Enzyme kinetics of purified PTE mutants.*** The evolved clone, PTE^{F9}, (blue circles), was compared to its parent enzyme, PTE^{R8} (green squares). Substrate inhibition was taken into account for PTE^{F9} (by fitting to the equation $v=v_{max}$ ([S]/{K_M + [S]+([S]^2/K_i}). The k_{cat}/K_m of PTE^{F9} was 19-fold improved compared to PTE^{R8} for turnover of substrate **1b** and 8-fold for its native substrate, paraoxon **1a**. The Michaelis-Menten parameters for turnover of paraoxon **1a**: PTE^{F9} (k_{cat}= 623 s^{-1}; K_M= 0.71 mM; k_{cat}/K_m = 8.8 x 10^5 M^{-1} s^{-1}; K_i= 0.46 mM); PTE^{R8} (k_{cat}= 67 s^{-1}; K_M= 0.6 mM; k_{cat}/K_m = 1.1 x 10^5 M^{-1} s^{-1}). **(b)** ***Turnover of***

substrate 1b by enzyme-loaded GSBs. *Left:* Schematic of the experimental set-up. Substrate **1a** is supplied in solution and added to a suspension of GSBs. When the substrate enters the GSBs that are filled with cell lysate or purified enzyme, catalysis occurs, yielding product **2a**. *Right:* Time courses of substrate hydrolysis ([**1a**] = 1 mM) catalyzed by purified PTE encapsulated in identical numbers of GSBs ([E] =70 nM inside GSBs that make up 10% of the total volume), reflecting the activity differences of evolved (blue circles: PTE^{F9}) and parental enzyme (green squares: PTE^{R8}). The control (purple triangles) consists of the supernatant from the wash of PTE^{F9} GSBs. *Conditions*: pH 7.5, T = 30 °C.